Immunobiology 222 (2017) 31–38

Contents lists available at ScienceDirect

Immunobiology

journal homepage: www.elsevier.com/locate/imbio

CD68+, but not stabilin-1+ tumor associated macrophages in gaps of ductal tumor structures negatively correlate with the lymphatic metastasis in human breast cancer

Mikhail Buldakov[a,b,1], Marina Zavyalova[a,b,c,1], Nadezhda Krakhmal[a,c], Nadezhda Telegina[c], Sergei Vtorushin[a,c], Irina Mitrofanova[a], Vladimir Riabov[a,d], Shuiping Yin[d], Bin Song[d], Nadezhda Cherdyntseva[a,b], Julia Kzhyshkowska[a,d,e,*]

[a] Laboratory for Translational Cellular and Molecular Biomedicine, Tomsk State University, Pr. Lenina, 36, 634050 Tomsk, Russia
[b] Tomsk Cancer Research Institute, Per. Kooperativny, 5, 634050 Tomsk, Russia
[c] Siberian State Medical University, Moskovskiy Trakt, 2, 634050 Tomsk, Russia
[d] Department of Innate Immunity and Tolerance, Institute of Transfusion Medicine and Immunology, Medical Faculty Mannheim, University of Heidelberg, Theodor-Kutzer-Ufer 1-3, 68167 Mannheim, Germany
[e] German Red Cross Blood Service Baden-Württemberg—Hessen, Friedrich-Ebert Strasse 107, 68167 Mannheim, Germany

ARTICLE INFO

Article history:
Received 2 August 2015
Received in revised form 3 September 2015
Accepted 4 September 2015
Available online 8 September 2015

Keywords:
Tumor-associated macrophages
CD68
Stabilin-1
Intratumoral heterogeneity
Lymphatic metastasis
Breast cancer

ABSTRACT

Tumor associated macrophages (TAM) support tumor growth and metastasis in several animal models of breast cancer, and TAM amount is predictive for efficient tumor growth and metastatic spread via blood circulation. However, limited information is available about intratumoral TAM heterogeneity and functional role of TAM subpopulations in tumor progression. The aim of our study was to examine correlation of TAM presence in various morphological segments of human breast cancer with clinical parameters. Thirty six female patients with nonspecific invasive breast cancer T1-4N0-3M0 were included in the study. Morphological examination was performed using Carl Zeiss Axio Lab.A1 and MiraxMidiZeiss. Immunohistochemical and immunofluorescence/confocal microcopy analysis was used to detect CD68 and stabilin-1 in 5 different tumor segments: (1) areas with soft fibrous stroma; (2) areas with coarse fibrous stroma; (3) areas of maximum stromal-and-parenchymal relationship; (4) parenchymal elements; (5) gaps of ductal tumor structures. The highest expression of CD68 was in areas with soft fibrous stroma or areas of maximum stromal-and-parenchymal relationship (79%). The lowest expression of CD68 was in areas with coarse fiber stroma (23%). Inverse correlation of tumor size and expression of CD68 in gaps of tubular tumor structures was found ($R = -0.67$; $p = 0.02$). In case of the lymph node metastases the average score of CD68 expression in ductal gaps tumor structures was lower (1.4 ± 0.5) compared to negative lymph nodes case (3.1 ± 1.0; $F = 10.9$; $p = 0.007$). Confocal microscopy identified 3 phenotypes of TAM: $CD68^+$/stabilin-1^-; $CD68^+$/stabilin-1^+ (over 50%); and $CD68^-$/stabilin-1^+. However, expression of stabilin-1 did not correlate with lymph node metastasis. We concluded, that increased amount of CD68+TAM in gaps of ductal tumor structures is protective against metastatic spread in regional lymph nodes.

Abbreviations: ANOVA, analysis of variance; BSA, bovine serum albumin; CCL, CC chemokine ligand; Cy, cyanine; ECM, extracellular matrix; EGF, epidermal growth factor; ER, estrogen receptor; HER2, human epidermal growth factor receptor 2; HRP, horseradish peroxidase; IHC, immunohistochemistry; IL, interleukin; LN, lymph node; MMP, matrix metalloproteinase; TAM, tumor associated macrophages; uPA, urokinase-type plasminogen activator; VEGF, vascular endothelial growth factor.

* Corresponding author at: Department of Innate Immunity and Tolerance, Institute of Transfusion Medicine and Immunology, Medical Faculty Mannheim, Heidelberg University, Theodor-Kutzer Ufer 1-3, D-68167 Mannheim, Germany. Fax: +49 621 383 9721.
E-mail addresses: julia.kzhyshkowska@medma.uni-heidelberg.de, julia.kzhyshkowska@gmail.com, julia.kzhyshkowska@umm.de (J. Kzhyshkowska).
1 Michael Buldakov and Marina Zavyalova contribute equally to this study.

http://dx.doi.org/10.1016/j.imbio.2015.09.011

1. Introduction

The supportive role of tumor associated macrophages (TAM) for tumor progression was primarily demonstrated in animal breast cancer models (Noy and Pollard, 2014). It was established that TAM belong to alternatively activated macrophages and can support tumor growth and metastasis using multiple mechanisms. For instance, TAM support survival and induce motility of breast cancer cells by producing epidermal growth factor (EGF) (Goswami et al., 2005). In spontaneous and ectopic models of breast cancer TAM produce pro-angiogenic factors such as VEGF-A contributing to angiogenesis and progression to malignancy, tumor cell growth and dissemination (Noy and Pollard, 2014; Gazzaniga et al., 2007; Lin et al., 2006; Sierra et al., 2008). Simultaneously with release of pro-angiogenic factors, the ability of TAM to produce matrix-degrading enzymes (MMP-2, MMP-9, uPA, cathepsins) and tumor cell-recruiting factors such as CCL-18 is associated with stimulation of breast tumor cell invasiveness and metastatic spread (Chen et al., 2011; Gocheva et al., 2010; Qian and Pollard, 2010). Moreover, TAM closely associate with blood vessels and promote tumor cells intravasation resulting in their escape into circulation and formation of distant metastases (Qian and Pollard, 2010; Pollard, 2008; Wyckoff et al., 2007).

However, in humans, not only positive but also negative correlations between TAM and various parameters of tumor growth and spread were demonstrated indicating much more complex mechanism of tumor cell-microenvironmental crass-talk. TAM density in different cancers is associated with incidence of distant metastases. TAM infiltration has positive or inverse correlation with metastases depending on tumor type. For example, high infiltration by CD68+ TAM was associated with higher risk of distant metastases in triple-negative breast cancer (Yuan et al., 2014). In addition, higher numbers of histological structures named tumor microenvironment for metastasis (TMEM) that represent close association of CD68+ macrophages, endothelial, and invasive tumor cells was associated with higher risk of distant metastasis in ER+/HER2–breast cancer (Rohan et al., 2014). In contrast, TAM infiltration was associated with suppression of metastases in high grade osteosarcoma (Buddingh et al., 2011). Similarly, higher density of CD68+ TAM was associated with lower incidence of hepatic metastases in colon cancer (Zhou et al., 2010).

In terms of lymphatic metastasis, mostly supportive role of TAM was demonstrated. For example, positive correlation between overall density of CD68+ TAM and lymph node (LN) metastases was found in human papillary thyroid carcinoma, endometrial cancer, cervical cancer, pulmonary adenocarcinoma, gastric cancer, breast cancer and others (Ding et al., 2012; Ohno et al., 2004; Qing et al., 2012; Riabov et al., 2014; Schoppmann et al., 2002; Takanami et al., 1999; Wu et al., 2012). Detrimental role of TAM in lymphatic metastases was mainly associated with their ability to produce pro-lymphangiogenic factors VEGF-C and VEGF-D that induce growth of intratumoral lymphatic vessels (Riabov et al., 2014; Iwata et al., 2007; Schoppmann et al., 2006; Song et al., 2013; Yang et al., 2011). They also release matrix-remodeling enzymes including MMP-2, MMP-9, and urokinase plasminogen activator (uPA) known to contribute to lymphangiogenesis (Riabov et al., 2014). Pro-lymphangiogenic and pro-metastatic properties of TAM were linked to their M2-like phenotype with preferential production of IL-10, CCL-18, and CCL-22 (Chen et al., 2011; Qing et al., 2012; Tsujikawa et al., 2013).

However, in the majority of studies only overall density of CD68+ TAM was analyzed and associated with LN metastases (Riabov et al., 2014). Insufficient attention was given to the intratumoral heterogeneity of TAM subtypes, in particular in relation to the different intratumoral structures. In human breast cancer following intratumoral compartments can be defined: (1) areas with soft fibrous stroma characterized by pronounced inflammatory infiltrates that are beneficial for invasive cell growth (Ham and Moon, 2013); (2) areas with coarse fibrous stroma containing collagen fibers and characterized by impaired synthesis of extracellular matrix proteins (ECM) (Campbell et al., 2011; Eiro et al., 2012; Ruffell et al., 2012; Tang, 2013); (3) areas of maximum stromal-and-parenchymal relationship revealing certain similarities with soft fibrous stroma (Mahmoud et al., 2012); (4) parenchymal elements; (5) gaps of ductal tumor structures (Pinder, 2010). All five stromal subtypes demonstrate functionally distinct areas of tumor mircoenvironment with not yet identified mechanistic role in metastatic spread.

In the present study we assessed the distribution of TAM in five distinct intratumoral morphological compartments and examined the correlation with clinical parameters of tumor progression. For the first time we demonstrated that amount of CD68+ macrophages in gaps of tubular tumor structures has negative correlation with lymph node metastasis. The highest amount of CD68+macrophages was present in the areas of soft fibrous stroma or areas of maximum stromal-and-parenchymal relationship (79%). We also identified three phenotype of TAM: $CD68^+$/stabilin-1^-; $CD68^+$/stabilin-1^+ (over 50%); and $CD68^-$/stabilin-1^+. However, expression of stabilin-1 did not correlate with lymph node metastasis. Our data suggested that increased amount of CD68 + TAM in gaps of ductal tumor structures is protective against metastatic spread in regional lymph nodes, and that these metastasis-protective TAM do not depend on pronounced M2-like activation.

2. Materials and methods

2.1. Patients

Thirty six female patients with nonspecific invasive breast cancer T1-4N0-3M0, who were treated in General Oncology Department of Tomsk Cancer Research Institute (Tomsk, Russia) from January 1999 to January 2007, were included in the present study. The study was approved by the Local Committee for Medical Ethics of our Institute (protocol No. 13 from 09.27.2014), and informed consents were obtained from all patients prior to analysis. Patients did not receive preoperative treatment. The mean age of women with breast cancer was 60.8 ± 11.3 years. Menstrual function was preserved in 7 (19%) patients, 29 women (81%) had menopause. The histological type of breast cancer was defined according to the WHO recommendations (Geneva, 2012) and corresponded to nonspecific invasive carcinoma in all cases.

2.2. Antibodies

The following primary antibodies were used: mouse monoclonal anti-human CD68 (BD Biosciences) and rabbit polyclonal anti-stabilin-1 RS1 (Kzhyshkowska et al., 2008). Super Sensitive Polymer-HRP detection system was used for immunohistochemical analysis (BioGenex, USA). Secondary antibodies for immunofluorescent staining were conjugated with Alexa488 (anti-mouse) and with Cy3 (anti-rabbit) (Dianova).

2.3. Immunohistochemical analysis

Fresh tumor tissues were fixed in 10% neutral formalin (Karbolit, Russia) for 24 h, rinsed with mixture of isopropanol (Biovitrum, Russia), and embedded in paraffin (Biovitrum, Russia). The antigen unmasking was performed using the PT Link module (Dako, Denmark) in a buffer with a high pH value. To visualize the antigen-antibody reaction, the Super Sensitive Polymer-HRP detection system was used (BioGenex, USA). Immunohistochemical analysis was performed by light microscope «Carl Zeiss Axio Lab.A1»

(Jenamed, Carl Zeiss, Germany) and slidescanner «MiraxMidiZeiss» (Germany). The results of the immunohistochemical analysis were assessed as the percentage of positively stained cells with any degree of positive marker expression in different parts of the section (1000 cells in 10 fields of view). Positive expression was determined by a 4-point scale: 1 point (+) – 1– cells in the view field; 2 points (++) – 3–5 cells in the view field; 3 points (+++) – 6–10 cells in the view field and 4 points (++++) – more than 10 cells in the view field (×400)

2.4. Digital IHC analysis and quantification

Tumor slides were scanned using the NIS Elements Imaging Software (Nikon, Japan). The Aperio ImageScope software (free from Aperio.com) was used to analyze and quantify marker expression. Individual tumor regions were selected and analyzed using the positive pixel count algorithm. The ImageScope software makes it possible to set the threshold for color saturation, as well as the upper and lower limits for the intensities of the weak- and strong-positive pixels. These thresholds were set using positive and negative control tissues. The results of analysis presented as positivity (number of positive pixels in a selected region to number of all pixels). Total number of analyzed samples were 24 for CD68 and 33 for RS1.

2.5. Immunofluorescent staining and confocal microscopy

Deparaffinization was performed with xylene and ethanol. Samples were blocked with 3% BSA in PBS, incubated with a combination of primary antibodies for 1 h, 15 min, washed, and incubated with a combination of appropriate secondary antibodies. Anti-CD68 and anti-stabilin-1 primary antibodies were used at a 1:100 and 1:1000 dilution correspondingly. Anti-mouse Alexa488 labeled and anti-rabbit Cy3 were used at 1:100 dilution. Samples were mounted with immunofluorescence mounting medium (DakoCytomation, Carpinteria, CA) and analyzed by confocal microscopy.

Confocal laser-scanning microscopy was performed using a Leica TCS SP2 laser-scanning spectral confocal microscope and Carl Zeiss LSM 780 NLO. Excitation was with an argon laser, emitting 488 nm; a krypton laser, emitting at 568 nm; and a helium/neon laser, emitting at 633 nm. Data were acquired and analyzed with Leica confocal software. All two- or three-color images were acquired using a sequential scan mode.

2.6. Statistical analysis

Statistical analysis was performed using STATISTICA 8.0 for Windows (StatSoft Inc., USA). The ANOVA, Chi-square test and Spearman correlation analysis were implemented. Statistical significance was set at p value <0.05, with a two-tail approach. Data with marginal significance (p value <0.1) were also discussed.

3. Results

3.1. Subpopulations of TAM in human breast cancer according to CD68 and stabilin-1 expression

It is widely accepted that tumor cells program TAM to acquire tolerogenic M2-like phenotype in order to inhibit anti-tumor immune responses and to promote tumor growth and metastasis. Stabilin-1 was shown by us to be marker for M2-type of macrophages that mediates clearance of unwanted-self components (Kzhyshkowska et al., 2008; Kzhyshkowska et al., 2006b; reviewed in Kzhyshkowska, 2010; Kzhyshkowska et al., 2006a). Therefore we examined whether TAM in human breast cancer express stabilin-1 on CD68+ macrophages. Using double immunofluorescence and confocal microscopy we demonstrated that stabilin-1 is abundantly expressed in TAM; and according to the CD68 and stabilin-1 positivity we could distinguish 3 subpopulations of TAM: $CD68^+$/stabilin-1^-; $CD68^+$/ stabilin-1^+; and $CD68^-$/ stabilin-1^+ (Fig. 1, Supplementary Fig. S1). Majority of macrophages were $CD68^+$, while around 50% of macrophages expressed stabilin-1. Therefore further quantitative immunohistochemical evaluation of the correlation of CD68 and stabilin-1, present in distinct morphological structures with clinical parameters has been performed separately for CD68 and for stabilin-1.

3.2. CD68 and stabilin-1 expression in five distinct intratumoral compartments of nonspecific invasive breast cancer

In order to examine whether CD68+ and stabilin-1+ TAM are differentially presented in five intratumoral compartments of breast cancer, immunohistochemical analysis of paraffin-embedded sections obtained from thirty six female patients with nonspecific invasive breast cancer was performed**.** We examine amounts of CD68+ and stabilin-1+ cells in following morphologically and functionally distinct areas of tumors (1) in areas with soft fibrous stroma (Fig. 2); (2) in areas with coarse fibrous stroma (Fig. 3); (3) in the areas of the so-called “maximum stromal-and-parenchymal relationship” where the individual tumor cells, short strands and groups of tumor cells arranged in soft fibrous stroma (Fig. 4); (4) among parenchymal elements (Fig. 5); (5) in gaps of ductal tumor structures (Fig. 6).

The highest expression (4 points or ++++) of CD68 in the inflammatory cell infiltrate was detected most frequently in areas with soft fibrous stroma (54% of analysed patients) or the so-called “maximum stromal-and-parenchymal relationship” (79%) in patients with breast cancer. The lowest expression (1 point or +) of CD68 was observed more frequently in areas with coarse fiber stroma (23%). The CD68-positive cells of the inflammatory infiltrate were absent often between parenchymal elements of tumor (88%) (Table 1, Figs. 2–6). For stabilin-1, the highest expression was found in maximum stromal-and-parenchymal relationship (44%), and the lowest in coarse fibrous stroma (13%), indicating that CD68 and stabilin-1 independently correlate with intratumoral morphological compartments (Table 2, Figs. 2–6).

3.3. Association of CD68 and stabilin-1 in five distinct intratumoral compartments and parameters of tumor growth

In order to examine the correlation between amount of CD68+ and stabilin-1+ cells in distinct intratumoral compartments, tumors size and grade of tumor malignancy were examined. We found inverse correlation ($R = -0.67$; $p = 0.02$) between tumor size and the expression of CD68 in the cells of the inflammatory infiltrate in gaps of tubular tumor structures (Table 3). The CD68 expression in the inflammatory cell infiltrate of the other tumor areas did not show significant correlation with tumor size (Table 3). No significant correlation was found between the CD68 expression in the inflammatory cell tumor infiltrate and the rate of tumor malignancy (Table 4). Presence of stabilin-1+ cells also had no significant correlation with tumor size or malignancy.

3.4. Correlation of CD68 and stabilin-1 with lymphatic metastasis

In order to further asses the role of TAM in progression of breast cancer we evaluated correlation with CD68+ and stabilin-1+ cells in lymphatic metastasis by detecting metastatic lesion in distant lymph nodes. We found, that amount of CD68+ TAM negatively correlated with the presence of metastatic regional lymph nodes. In the case of the lymph node metastases the average score of CD68 expression in cells of ductal gaps tumor structures was

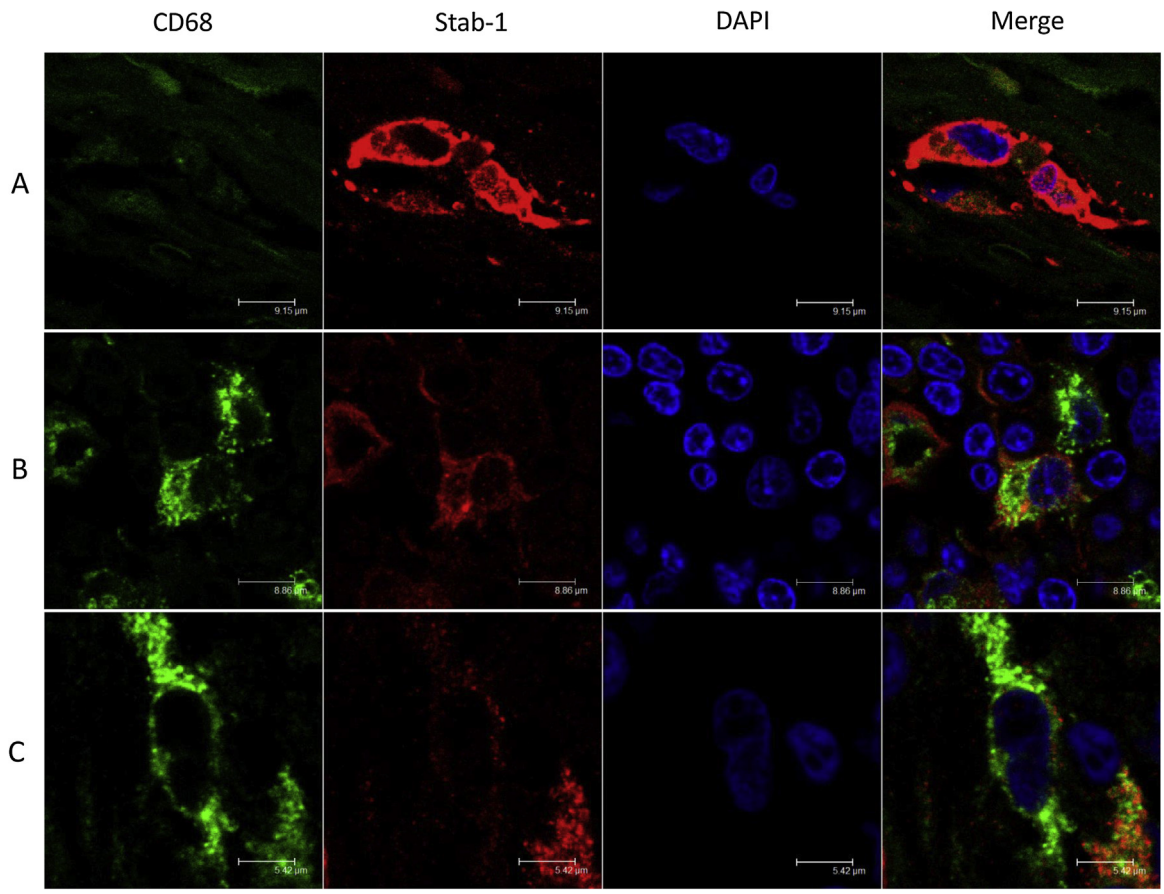

Fig. 1. Subpopulations of CD68+ and stabilin-1+ TAM in patients with nonspecific invasive breast carcinoma. CD68 was detected by immunofluorescent staining using a-CD68 mouse primary antibody and Alexa488- conjugated anti-mouse antibody (shown in green), stabilin-1 was detected by RS1 rabbit polyclonal primary antibody and Cy3-conjugated anti-rabbit secondary antibody (shown in red). Visualization of nuclei was performed using Dapi. Representative images are shown for CD68-/stabilin-1+ (A), CD68+/stabilin-1- and CD68+/stabilin-1+ (B and C) subpopulations. Scale bars: 9,15 μm (A); 8,86 μm (B); and 5,42 μm (C).

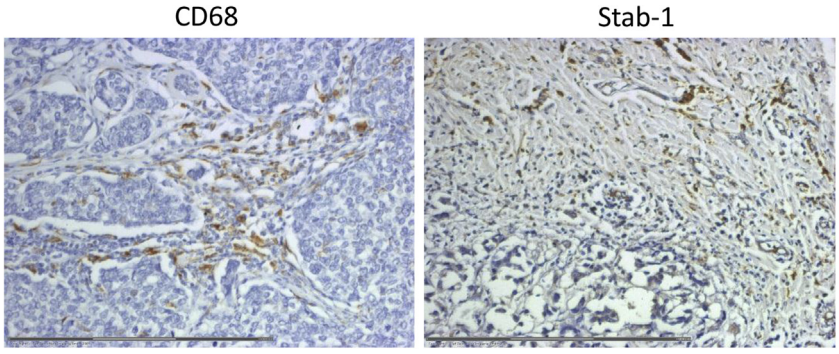

Fig. 2. Immunohistochemical analysis of CD68 and stabilin-1 expression in intratumoral compartment with soft fiber stroma in patients ($n = 36$) with nonspecific invasive breast carcinoma. CD68 was visualized using mouse monoclonal antibody (Novocastra, clone 514H12). Stabilin-1 was visualized using rabbit polyclonal RS1 antibody. Visualization of nuclei was performed using hematoxylin. Representative image from one patient is shown. Scale bar 300 μm (×400).

lower (1.4 ± 0.5) in comparison with the negative lymph nodes case (3.1 ± 1.0; $F = 10.9$; $p = 0.007$) (Table 5). Amount of stabilin-1+ cells did not show significant correlation with the presence of lymphatic metastasis.

In order to verify the negative correlation of CD68+ TAM with lymphatic metastasis, we applied quantitative digital immunohistology using Nikon Eclipse Ni Microscop and Aperio ImageScope software. The Positivity of CD68 in gaps of ductal tumor structures was higher (0.34 ± 0.4) for patients without lymph node metastases compared to patients with lymphatic metastasis (0.1 ± 0.1). There were no significant difference in the presence of stabilin-1+ TAM in tumor section obtained from patients with or without lymph node metastasis (0.05 ± 0.18 and 0.06 ± 0.2 correspondently) (Table 6). Thus, the results of quantitative ImageScope analysis confirmed the results of conventional immunohistological quantification (Tables 5 and 6). For the first time it was demonstrated that the presence of CD68+ TAM in ductal tumor structures has negative effect on the metastatic spread via lymphatic pathway in breast cancer patients. Moreover, this effect was independent of M2 phenotype acquisition.

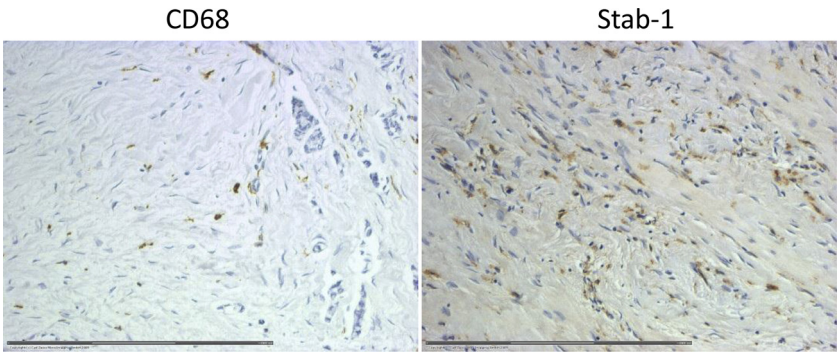

Fig. 3. Immunohistochemical analysis of CD68 and stabilin-1 expression in intratumoral compartment with coarse fiber stroma in patients ($n = 36$) with nonspecific invasive breast carcinoma. CD68 was visualized using mouse monoclonal antibody (Novocastra, clone 514H12). Stabilin-1 was visualized using rabbit polyclonal RS1 antibody. Visualization of nuclei was performed using hematoxylin. Representative image from one patient is shown. Scale bar 300 μm (×400).

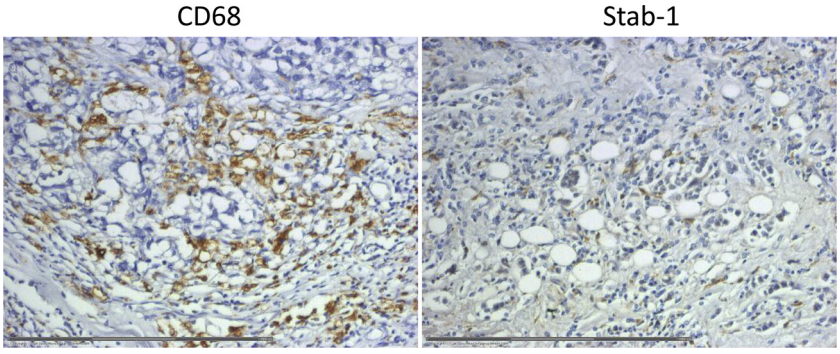

Fig. 4. Immunohistochemical analysis of CD68 and stabilin-1 expression in the intratumoral compartment with "maximum stromal and parenchymal cooperation" in patients ($n = 36$) with nonspecific invasive breast carcinoma. Representative image is demonstrated. CD68 was visualized using mouse monoclonal antibody (Novocastra, clone 514H12). Stabilin-1 was detected using rabbit polyclonal RS1 antibody. Visualization of nuclei was performed using hematoxylin. Representative image from one patient is shown. Scale bar 300 μm (×400).

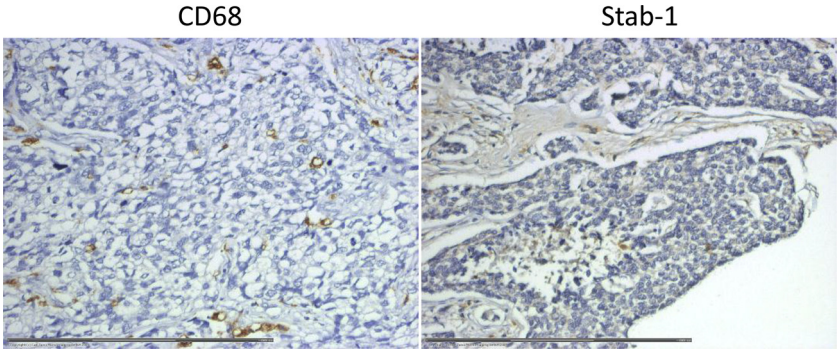

Fig. 5. Immunohistochemical analysis of CD68 and stabilin-1 expression intratumoral compartment between parenchymal structures in patients ($n = 36$) with nonspecific invasive breast carcinoma. Representative image is demonstrated. CD68 was detected using mouse monoclonal antibody (Novocastra, clone 514H12). Stabilin-1 was detected using rabbit polyclonal RS1 antibody. Visualization of nuclei was performed using hematoxylin. Representative image from one patient is shown. Scale bar 300 μm (×400).

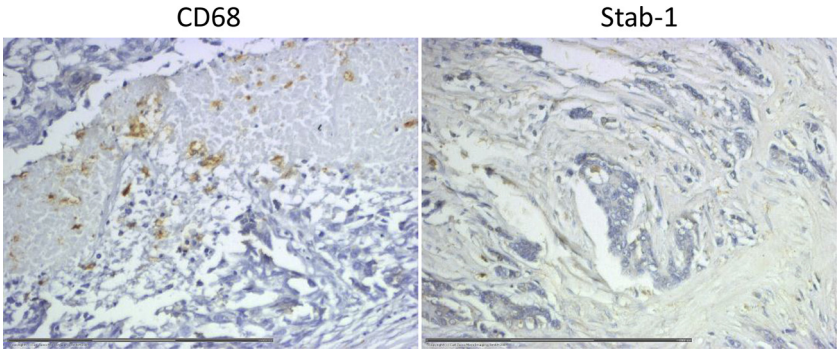

Fig. 6. Immunohistochemical analysis of CD68 and stabilin-1 expression in inflammatory infiltrate cells in gaps of ductal-like structures in patients ($n = 36$) with nonspecific invasive breast carcinoma. CD68 was visualized using mouse monoclonal antibody (Novocastra, clone 514H12). Stabilin-1 was visualized using Stabilin-1 was detected using rabbit polyclonal RS1 antibody. Visualization of nuclei was performed using hematoxylin. Representative image from one patient is shown. Scale bar 300 μm (×400).

Table 1
The CD68 expression in the inflammatory cell infiltrate in patients with the nonspecific invasive breast cancer.

Localization		CD68 expression, the number of patients, in abs. (%)				
		No	1 point	2 points	3 points	4 points
In soft fibrous stroma	1	4/35 (11%)	1/35 (3%)	8/35 (23%)	3/35 (9%)	19/35 (54%) $p_2 = 0.0001$ $p_4 = 0.0000$ $p_5 = 0.0002$
In coarse fibrous stroma	2	6/31 (19%)	7/31 (23%) $p_1 = 0.008$ $p_5 = 0.06$	12/31 (39%)	3/31 (9.5%)	3/31 (9.5%)
"Maximum stromal-and-parenchymal relationship"	3	1/14 (7%)	–	1/14 (7%)	1/14 (7%)	11/14 (79%) $p_2 = 0.0000$ $p_4 = 0.0000$ $p_5 = 0.0000$
Among parenchymal elements	4	32/36 (88%) $p_1 = 0.0000$ $p_2 = 0.0000$ $p_3 = 0.0000$	–	1/36 (3%)	1/36 (3%)	2/36 (6%)
In gaps of ductal tumor structures	5	22/34 (65%)	3/34 (9%)	5/34 (14%)	–	4/34 (12%)

Table 2
Expression of stabilin-1 in the inflammatory cell infiltrate in patients with the nonspecific invasive breast cancer.

Localization		Stabilin-1 expression, the number of patients, in abs. (%)				
		No	1 point	2 points	3 points	4 points
In soft fibrous stroma	1	13/35 (37%)	2/35 (6%)	8/35 (23%)	5/35 (14%)	7/35 (20%)
In coarse fibrous stroma	2	20/31 (63%) $p_1 = 0{,}01$	4/31 (13%)	3/31 (9%)	2/31 (6%)	3/31 (9%)
"Maximum stromal-and-parenchymal relationship"	3	4/9 (44%)	1/9 (12%)	–	–	4/9 (44%) $p_1 = 0{,}07$ $p_2 = 0{,}009$ $p_5 = 0{,}001$
Among parenchymal elements	4	33/36 (91%) $p_1 = 0{,}0000$ $p_3 = 0{,}001$	2/36 (6%)	1/36 (3%)	–	–
In gaps of ductal tumor structures	5	27/30 (90%) $p_1 = 0{,}0000$ $p_3 = 0{,}002$	2/30 (6,5%)	–	–	1/30 (3,5%)

Table 3
The correlation of CD68 and stabilin-1 expression with tumor size in patients with the nonspecific invasive breast cancer.

Macrophage marker expression	Tumor size	
	CD68	Stabilin-1
In soft fibrous stroma	$R = 0.06$; $p = 0.72$ ($n = 29$)	$R = 0.39$; $p = 0.06$ ($n = 22$)
In coarse fibrous stroma	$R = 0.19$; $p = 0.35$ ($n = 24$)	$R = 0.27$; $p = 0.89$ ($n = 12$)
"Maximum stromal-and-parenchymal relationship"	$R = 0.08$; $p = 0.78$ ($n = 12$)	$R = -0.35$; $p = -0.65$ ($n = 5$)
Among parenchymal elements	$R = -0.94$; $p = -4.24$ ($n = 4$)	$R = 0.86$; $p = 1.73$ ($n = 3$)
In gaps of ductal tumor structures	$R = -0.67$; $p = 0.02$ ($n = 11$)	$R = 0.5$; $p = 0.58$ ($n = 3$)

Table 4
The correlation of CD68 expression in the inflammatory cell infiltrate with the rate of tumor malignancy in patients with the nonspecific invasive breast cancer.

Macrophage marker expression	The rate of tumor malignancy	
	CD68	Stabilin-1
In soft fibrous stroma	$R = 0.19$; $p = 0.35$ ($n = 25$)	$R = 0.21$; $p = 0.93$ ($n = 20$)
In coarse fibrous stroma	$R = -0.20$; $p = -0.86$ ($n = 20$)	$R = -0.23$; $p = -0.72$ ($n = 11$)
"Maximum stromal-and-parenchymal relationship"	$R = 0.52$; $p = 0.92$ ($n = 9$)	$R = 0.18$; $p = 0.32$ ($n = 5$)
Among parenchymal elements	$R = 0.54$; $p = 0.92$ ($n = 4$)	$R = -1.0$ ($n = 3$)
In gaps of ductal tumor structures	$R = 0.55$; $p = 1.90$ ($n = 10$)	$R = 1.0$ ($n = 3$)

4. Discussion

Tumor associated macrophages are traditionally believed to possess mostly tumor supporting role. Studies in animal models revealed that TAM release factors that stimulate angiogenic switch and lymphatic vessel growth (Lin et al., 2006; Riabov et al., 2014; Iwata et al., 2007; Lin et al., 2007; Yeo et al., 2014). However, accumulating data indicate that in human patients amount of TAM can also negatively correlate with parameters of tumor progression (Buddingh et al., 2011; Zhou et al., 2010, Forssell et al., 2007; Ohri et al., 2009).

Table 5
Immonohistological assessment of the correlation of CD68+ and stabilin-1+ TAM with lymphatic metastasis in patients with the nonspecific invasive breast cancer.

Localization	The average score of CD68 expression, M±SD		The average score of stabilin-1 expression, M ± SD	
	N0	N+	N0	N+
in soft fibrous stroma	3.5 ± 0.8 (n = 20)	2.8 ± 0.8 (n = 10) F = 3.7; p = 0.06	2.7 ± 1.1 (n = 16)	3.0 ± 0.8 (n = 6) F = 0,39; p = 0.53
in coarse fibrous stroma	2.2 ± 0.9 (n = 17)	1.7 ± 1.1 (n = 7) F = 1.4; p = 0.24	2.2 ± 1.2 (n = 9)	2.7 ± 1.5 (n = 3) F = 0.27; p = 0.61
"maximum stromal-and-parenchymal relationship"	4.0 ± 0.0 (n = 8)	3.5 ± 1.0 (n = 4) F = 2.2; p = 0.16	3.4 ± 1.3 (n = 5)	−(n = 0)
among parenchymal elements	3.3 ± 1.1 (n = 3)	3.0 (n = 1) F = 0.06; p = 0.82	1.3 ± 0.3 (n = 3)	−(n = 0)
in gaps of ductal tumor structures	3.1 ± 1.0 (n = 7)	1.4 ± 0.5 (n = 5) F = 10.9; p = 0.007	2.5 ± 2.1 (n = 2)	1.0 (n = 1) F = 0.33; p = 0.66

Table 6
The correlation of CD68 expression in gaps of ductal tumor structures of the inflammatory cell infiltrate with lymphatic metastasis quantified by ImageScope software.

Lymphogenous metastasis	CD68 (mean ± SD) p = 0.001	Stabilin-1 (mean±SD) p = 0.93
N0	0.34 ± 0.4	0.06 ± 0.2
N1	0.1 ± 0.1	0.05 ± 0.18

Our study for the first time assessed amount of TAM in five distinct morphological compartments of human breast cancer and demonstrated that amount of TAM in the gaps of ductal tumor structures is associated not with increased, but with decreased ability of tumor to metastasize into lymphatic nodes.

The amounts of TAM, expressing CD68 and stabilin-1 (marker of alternative macrophage activation) (Kzhyshkowska, 2010; Kzhyshkowska et al., 2006a,b) have been evaluated separately, since we showed using immunofluorescent staining and confocal microscopy, that presence of these two markers only partially overlap on TAM, and cells expressing only CD68 or only stabilin-1 may constitute around half of total TAM population in breast cancer.

The principal issue of our study was the analysis of TAM in distinct morphological structures, where morphology can be also linked to the functional characteristics of these tumor areas.

In human breast cancer five distinct intratumoral compartments can be defined. First structure is represented by areas with soft fibrous stroma that are in general characterized by pronounced inflammatory infiltrates. Stroma has soft fibrous, reticular composition with the presence of large multicellular complexes (solid, alveolar structures). This type of stroma is beneficial for invasive cell growth (Ham and Moon, 2013). Identified high amounts of CD68+ and stabilin-1+ TAM in the areas with soft fibrous stroma can be explained by pronounced infiltration due to the reticular morphology that allows formation of multicellular complexes.

Second intratumoral compartment includes areas with coarse fibrous stroma that contain collagen fibers and often reveal signs of hyalinosis. Coarse stroma progressively loses normal functions due to impaired synthesis of extracellular matrix proteins (ECM). As a result, presentation of bioactive molecules to the cells is strongly decreased. Moreover, vascular network, leukocyte extravasation and motility are impaired in coarse stroma (Campbell et al., 2011; Eiro et al., 2012; Ruffell et al., 2012; Tang, 2013). In accordance to these features we found significantly less of both CD68+ and stabilin-1+ TAM in coarse fibrous stroma compared to their high amounts in areas with soft fibrous stroma.

High amounts of CD68+ and stabilin-1+ TAM were found it the third intratumoral compartment—areas of maximum stromal-and-parenchymal relationship revealing some similarities with soft fibrous stroma. In these areas short fibers and discrete groups of cells can be found in the context of soft fibrous reticular stroma enabling efficient binding of cytokines and growth factors by ECM and their presentation to cells for optimal cell-stroma interactions (Mahmoud et al., 2012), supporting the accumulation of TAM.

Amount of TAM is significantly lower in the fourth intratumoral compartment—parenchymal elements, where presence of single TAM can be explained by general ability of monocyte-derived cells to infiltrate into the areas with signs of chronic inflammation (Lofdahl et al., 2012). In our study the amount of TAM in parenchymal elements showed no relations to the parameters of tumor growth.

Finally, fifth compartment includes gaps of ductal tumor structures, which are the sites of primary proliferation of atypical and malignant epithelial cells. The striking findings were the identification made both by conventional quantitative immunohistology and digital quantification of the negative correlation of increased amounts of CD68+ TAM with lymphatic metastasis. Similar finding has been recently published for colorectal cancer. Thus, in contrast to vast majority of studies demonstrating positive association between high TAM infiltration and LN metastases, low numbers of CD68+ TAM in tumor invasive front were associated with presence of LN metastases in colorectal cancer patients suggesting that TAM subpopulations localized in certain tumor areas are able to delay LN metastases at least in certain types of cancer (Gulubova et al., 2013).

Negative correlation of increased amount of CD68+TAM in our analysis of breast cancer samples can be explained by the ability of macrophages that are not yet re-programmed by tumor cells and possess normal migration capacities to infiltrate into ductal structures. The fact that association of CD68+TAM in ductal structures with decreased lymphatic metastasis is independent on expression of M2-marker stabilin-1 further supports the hypothesis that ductal TAM are not completely programmed by tumor cells to be highly tolerogenic and supporting tumor progression including lymphatic metastasis. Moreover, we can hypothesize that other anti-tumor activities might be found in the future in the ductal TAM that primarily attempt to recognize transformed cells and inhibit tumor progression at the place of origin. Most interesting will be identification in future the origin of these TAM that keep them open for plastic programming in response to tumor microenvironment.

Conflict of interest

None.

Acknowledgments

The study was supported by the Russian Scientific Foundation, grant #14-15-00350. Work was carried out on equipment of Tomsk

regional common use center, with the support of the Russian Ministry of the Agreement No.14.594.21.0001 (RFMEFI59414 × 0001).

Appendix A. Supplementary data

Supplementary data associated with this article can be found, in the online version, at http://dx.doi.org/10.1016/j.imbio.2015.09.011.

References

Buddingh, E.P., Kuijjer, M.L., Duim, R.A., Burger, H., Agelopoulos, K., Myklebost, O., Serra, M., Mertens, F., Hogendoorn, P.C., Lankester, A.C., Cleton-Jansen, A.M., 2011. Tumor-infiltrating macrophages are associated with metastasis suppression in high-grade osteosarcoma: a rationale for treatment with macrophage activating agents. Clin. Cancer Res. 17, 2110.

Campbell, M.J., Tonlaar, N.Y., Garwood, E.R., Huo, D., Moore, D.H., Khramtsov, A.I., Au, A., Baehner, F., Chen, Y., Malaka, D.O., Lin, A., Adeyanju, O.O., Li, S., Gong, C., McGrath, M., Olopade, O.I., Esserman, L.J., 2011. Proliferating macrophages associated with high grade, hormone receptor negative breast cancer and poor clinical outcome. Breast Cancer Res. Treat. 128, 703.

Chen, J., Yao, Y., Gong, C., Yu, F., Su, S., Chen, J., Liu, B., Deng, H., Wang, F., Lin, L., Yao, H., Su, F., Anderson, K.S., Liu, Q., Ewen, M.E., Yao, X., Song, E., 2011. CCL18 from tumor-associated macrophages promotes breast cancer metastasis via PITPNM3. Cancer Cell 19, 541.

Ding, M., Fu, X., Tan, H., Wang, R., Chen, Z., Ding, S., 2012. The effect of vascular endothelial growth factor C expression in tumor-associated macrophages on lymphangiogenesis and lymphatic metastasis in breast cancer. Mol. Med. Rep. 6, 1023.

Eiro, N., Pidal, I., Fernandez-Garcia, B., Junquera, S., Lamelas, M.L., del Casar, J.M., Gonzalez, L.O., Lopez-Muniz, A., Vizoso, F.J., 2012. Impact of CD68/(CD3 + CD20) ratio at the invasive front of primary tumors on distant metastasis development in breast cancer. PLoS One 7, e52796.

Forssell, J., Oberg, A., Henriksson, M.L., Stenling, R., Jung, A., Palmqvist, R., 2007. High macrophage infiltration along the tumor front correlates with improved survival in colon cancer. Clin. Cancer Res. 13, 1472.

Gazzaniga, S., Bravo, A.I., Guglielmotti, A., van Rooijen, N., Maschi, F., Vecchi, A., Mantovani, A., Mordoh, J., Wainstok, R., 2007. Targeting tumor-associated macrophages and inhibition of MCP-1 reduce angiogenesis and tumor growth in a human melanoma xenograft. J. Invest. Dermatol. 127, 2031.

Gocheva, V., Wang, H.W., Gadea, B.B., Shree, T., Hunter, K.E., Garfall, A.L., Berman, T., Joyce, J.A., 2010. IL-4 induces cathepsin protease activity in tumor-associated macrophages to promote cancer growth and invasion. Genes Dev. 24, 241.

Goswami, S., Sahai, E., Wyckoff, J.B., Cammer, M., Cox, D., Pixley, F.J., Stanley, E.R., Segall, J.E., Condeelis, J.S., 2005. Macrophages promote the invasion of breast carcinoma cells via a colony-stimulating factor-1/epidermal growth factor paracrine loop. Cancer Res. 65, 5278.

Gulubova, M., Ananiev, J., Yovchev, Y., Julianov, A., Karashmalakov, A., Vlaykova, T., 2013. The density of macrophages in colorectal cancer is inversely correlated to TGF-beta1 expression and patients' survival. J. Mol. Histol. 44, 679.

Ham, M., Moon, A., 2013. Inflammatory and microenvironmental factors involved in breast cancer progression. Arch. Pharm. Res. 36, 1419.

Iwata, C., Kano, M.R., Komuro, A., Oka, M., Kiyono, K., Johansson, E., Morishita, Y., Yashiro, M., Hirakawa, K., Kaminishi, M., Miyazono, K., 2007. Inhibition of cyclooxygenase-2 suppresses lymph node metastasis via reduction of lymphangiogenesis. Cancer Res. 67, 10181.

Kzhyshkowska, J., 2010. Multifunctional receptor stabilin-1 in homeostasis and disease. Sci. World J. 10, 2039.

Kzhyshkowska, J., Gratchev, A., Goerdt, S., 2006a. Stabilin-1, a homeostatic scavenger receptor with multiple functions. J. Cell. Mol. Med. 10, 635.

Kzhyshkowska, J., Workman, G., Cardo-Vila, M., Arap, W., Pasqualini, R., Gratchev, A., Krusell, L., Goerdt, S., Sage, E.H., 2006b. Novel function of alternatively activated macrophages: stabilin-1-mediated clearance of SPARC. J. Immunol. 176, 5825.

Kzhyshkowska, J., Gratchev, A., Schmuttermaier, C., Brundiers, H., Krusell, L., Mamidi, S., Zhang, J., Workman, G., Sage, E.H., Anderle, C., Sedlmayr, P., Goerdt, S., 2008. Alternatively activated macrophages regulate extracellular levels of the hormone placental lactogen via receptor-mediated uptake and transcytosis. J. Immunol. 180, 3028.

Lin, E.Y., Li, J.F., Bricard, G., Wang, W., Deng, Y., Sellers, R., Porcelli, S.A., Pollard, J.W., 2007. Vascular endothelial growth factor restores delayed tumor progression in tumors depleted of macrophages. Mol. Oncol. 1, 288.

Lin, E.Y., Li, J.F., Gnatovskiy, L., Deng, Y., Zhu, L., Grzesik, D.A., Qian, H., Xue, X.N., Pollard, J.W., 2006. Macrophages regulate the angiogenic switch in a mouse model of breast cancer. Cancer Res. 66, 11238.

Lofdahl, B., Ahlin, C., Holmqvist, M., Holmberg, L., Zhou, W., Fjallskog, M.L., Amini, R.M., 2012. Inflammatory cells in node-negative breast cancer. Acta Oncol. 51, 680.

Mahmoud, S.M., Lee, A.H., Paish, E.C., Macmillan, R.D., Ellis, I.O., Green, A.R., 2012. Tumour-infiltrating macrophages and clinical outcome in breast cancer. J. Clin. Pathol. 65, 159.

Noy, R., Pollard, J.W., 2014. Tumor-associated macrophages: from mechanisms to therapy. Immunity 41, 49.

Ohno, S., Ohno, Y., Suzuki, N., Kamei, T., Koike, K., Inagawa, H., Kohchi, C., Soma, G., Inoue, M., 2004. Correlation of histological localization of tumor-associated macrophages with clinicopathological features in endometrial cancer. Anticancer Res. 24, 3335.

Ohri, C.M., Shikotra, A., Green, R.H., Waller, D.A., Bradding, P., 2009. Macrophages within NSCLC tumour islets are predominantly of a cytotoxic M1 phenotype associated with extended survival. Eur. Respir. J. 33, 118.

Pinder, S.E., 2010. Ductal carcinoma in situ (DCIS): pathological features, differential diagnosis, prognostic factors and specimen evaluation. Mod. Pathol. 23 (Suppl. 2), S8.

Pollard, J.W., 2008. Macrophages define the invasive microenvironment in breast cancer. J. Leukoc. Biol. 84, 623.

Qian, B.Z., Pollard, J.W., 2010. Macrophage diversity enhances tumor progression and metastasis. Cell 141, 39.

Qing, W., Fang, W.Y., Ye, L., Shen, L.Y., Zhang, X.F., Fei, X.C., Chen, X., Wang, W.Q., Li, X.Y., Xiao, J.C., Ning, G., 2012. Density of tumor-associated macrophages correlates with lymph node metastasis in papillary thyroid carcinoma. Thyroid 22, 905.

Riabov, V., Gudima, A., Wang, N., Mickley, A., Orekhov, A., Kzhyshkowska, J., 2014. Role of tumor associated macrophages in tumor angiogenesis and lymphangiogenesis. Front. Physiol. 5, 75.

Rohan, T.E., Xue, X., Lin, H.M., D'Alfonso, T.M., Ginter, P.S., Oktay, M.H., Robinson, B.D., Ginsberg, M., Gertler, F.B., Glass, A.G., Sparano, J.A., Condeelis, J.S., Jones, J.G., 2014. Tumor microenvironment of metastasis and risk of distant metastasis of breast cancer. J. Natl. Cancer Inst. 106.

Ruffell, B., Au, A., Rugo, H.S., Esserman, L.J., Hwang, E.S., Coussens, L.M., 2012. Leukocyte composition of human breast cancer. Proc. Natl. Acad. Sci. U. S. A. 109, 2796.

Schoppmann, S.F., Birner, P., Stockl, J., Kalt, R., Ullrich, R., Caucig, C., Kriehuber, E., Nagy, K., Alitalo, K., Kerjaschki, D., 2002. Tumor-associated macrophages express lymphatic endothelial growth factors and are related to peritumoral lymphangiogenesis. Am. J. Pathol. 161, 947.

Schoppmann, S.F., Fenzl, A., Nagy, K., Unger, S., Bayer, G., Geleff, S., Gnant, M., Horvat, R., Jakesz, R., Birner, P., 2006. VEGF-C expressing tumor-associated macrophages in lymph node positive breast cancer: impact on lymphangiogenesis and survival. Surgery 139, 839.

Sierra, J.R., Corso, S., Caione, L., Cepero, V., Conrotto, P., Cignetti, A., Piacibello, W., Kumanogoh, A., Kikutani, H., Comoglio, P.M., Tamagnone, L., Giordano, S., 2008. Tumor angiogenesis and progression are enhanced by Sema4D produced by tumor-associated macrophages. J. Exp. Med. 205, 1673.

Song, K., Herzog, B.H., Sheng, M., Fu, J., McDaniel, J.M., Chen, H., Ruan, J., Xia, L., 2013. Lenalidomide inhibits lymphangiogenesis in preclinical models of mantle cell lymphoma. Cancer Res. 73, 7254.

Takanami, I., Takeuchi, K., Kodaira, S., 1999. Tumor-associated macrophage infiltration in pulmonary adenocarcinoma: association with angiogenesis and poor prognosis. Oncology 57, 138.

Tang, X., 2013. Tumor-associated macrophages as potential diagnostic and prognostic biomarkers in breast cancer. Cancer Lett. 332, 3.

Tsujikawa, T., Yaguchi, T., Ohmura, G., Ohta, S., Kobayashi, A., Kawamura, N., Fujita, T., Nakano, H., Shimada, T., Takahashi, T., Nakao, R., Yanagisawa, A., Hisa, Y., Kawakami, Y., 2013. Autocrine and paracrine loops between cancer cells and macrophages promote lymph node metastasis via CCR4/CCL22 in head and neck squamous cell carcinoma. Int. J. Cancer 132, 2755.

Wu, H., Xu, J.B., He, Y.L., Peng, J.J., Zhang, X.H., Chen, C.Q., Li, W., Cai, S.R., 2012. Tumor-associated macrophages promote angiogenesis and lymphangiogenesis of gastric cancer. J. Surg. Oncol. 106, 462.

Wyckoff, J.B., Wang, Y., Lin, E.Y., Li, J.F., Goswami, S., Stanley, E.R., Segall, J.E., Pollard, J.W., Condeelis, J., 2007. Direct visualization of macrophage-assisted tumor cell intravasation in mammary tumors. Cancer Res. 67, 2649.

Yang, H., Kim, C., Kim, M.J., Schwendener, R.A., Alitalo, K., Heston, W., Kim, I., Kim, W.J., Koh, G.Y., 2011. Soluble vascular endothelial growth factor receptor-3 suppresses lymphangiogenesis and lymphatic metastasis in bladder cancer. Mol. Cancer 10, 36.

Yeo, E.J., Cassetta, L., Qian, B.Z., Lewkowich, I., Li, J.F., Stefater, J.A., Smith, 3rd, Wiechmann, A.N., Wang, L.S., Pollard, Y., Lang, J.W., 2014. Myeloid WNT7b mediates the angiogenic switch and metastasis in breast cancer. Cancer Res. 74, 2962.

Yuan, Z.Y., Luo, R.Z., Peng, R.J., Wang, S.S., Xue, C., 2014. High infiltration of tumor-associated macrophages in triple-negative breast is associated with a higher risk of distant metastasis. Oncol. Targets Ther. 7, 1475.

Zhou, Q., Peng, R.Q., Wu, X.J., Xia, Q., Hou, J.H., Ding, Y., Zhou, Q.M., Zhang, X., Pang, Z.Z., Wan, D.S., Zeng, Y.X., Zhang, X.S., 2010. The density of macrophages in the invasive front is inversely correlated to liver metastasis in colon cancer. J. Transl. Med. 8, 13.